Photolithographically definable SU-8–alumina composite for W-band dielectric resonator antennas

Najeeb Al-Khalli[1], Mohammad Alduraibi[2], Nacer Debbar[1], Muhammad Saleem[1], Majeed Alkanhal[1], Abdelrazik Sebak[3,4], Mohamed Abdel-Rahman[1]

[1]*Department of Electrical Engineering, College of Engineering, King Saud University, P.O. Box 800, Riyadh 11421, Saudi Arabia*
[2]*Physics and Astronomy Department, College of Science, King Saud University, P.O. Box 2455, Riyadh 11451, Saudi Arabia*
[3]*Electrical and Computer Engineering Department, Concordia University, Montreal, QC, Canada*
[4]*KACST Technology Innovation Center in RFTONICS, King Saud University, Riyadh 11421, Saudi Arabia*
E-mail: mabdelrahman@ksu.edu.sa

Published in Micro & Nano Letters; Received on 10th September 2015; Revised on 22nd February 2016; Accepted on 24th February 2016

A novel process has been developed for fabricating ceramic dielectric structures with dimensions applicable to W-band millimetre wave dielectric resonator antennas. The ceramic dielectric structures are based on composites of SU-8 2150 photoresist and alumina (Al_2O_3)-alpha nanopowder. The effects of increasing the weight percentage of Al_2O_3 nanopowder on the photo-polymerisation of the SU-8–Al_2O_3 composite were systematically investigated. Cylindrical structures with thicknesses up to 500 μm have been fabricated using single casted conventional ultraviolet lithography. The relative permittivity of SU-8–Al_2O_3 composites at different weight percentages of Al_2O_3 was studied showing an increase from a relative permittivity of 4.5 to 5.66 with increasing the Al_2O_3 weight percentage from 0 to 35%. Also, finally, double layer manufacturing of ceramic SU-8–Al_2O_3 composite structures was demonstrated.

1. Introduction: Dielectric resonator antennas (DRAs) have been widely investigated in microwave and millimetre wave (MMW) frequency bands due to several attractive properties [1, 2]. DRAs operating in the microwave and MMW frequency bands have shown high radiation efficiencies when compared to printed metallic antennas. This is mainly due to the absence of conductor and surface wave losses, which are greatly dominant in printed metallic antennas. In addition, DRAs can be designed in various shapes and can be configured to have different excitation modes and feeding schemes which offer great design flexibilities. However, as the frequency of operation increases, the realisation of a small size DRA becomes hard and expensive due to manufacturing complexities involved in micromachining the composing ceramic materials with small dimensions and acceptable dimensional tolerances and also due to the requirement of accurately positioning of the DRA structure with respect to the feed structure.

Recently, a new technique was conceived to manufacture low permittivity dielectric material using polymer–ceramic composites, which are being used in several applications, such as embedded capacitor [3], broadband acoustical matching [4], high voltage outdoor insulation [5] and packaging [6]. Different polymer material and ceramic composites were used depending on the application specifications. This technique has also been successfully used to manufacture low permittivity dielectric resonator antennas in the K-band [7–10]. A photoresist was used as a polymer with added ceramic microparticles used as filler to the polymer to increase the dielectric constant of the composite; therefore, yielding more efficient coupling between the dielectric resonator structure and its feed structure as well as reducing the antenna required size [1, 8]. The advantage of this technique is that it keeps the polymer flexibility, which makes it easy to shape, and gains at the same time some of the ceramic filler properties. The increase in polymer's dielectric constant was found to depend on the ceramic filler dielectric constant, its concentration in the composite mixture, and its average particle size [11].

In previous works [12], Rashidian *et al.* used direct [8, 13] and indirect [7] X-ray lithography to fabricate polymer–ceramic composited-based DRAs. In the direct method, polymer–ceramic composited-based was patterned using a mould technique followed by deep X-ray exposure, in the indirect method a precise permanent frame was fabricated by X-ray lithography then filled with polymer–ceramic mixture using robotic machine. In both techniques, the fabricated DRAs were aligned manually with signal feeding mechanism after demount them from the moulds. These techniques have proved successful in defining DRA in the K-band with a good control over the dielectric constant; however, for W-band MMW frequencies, these techniques will become limited in providing the required dimensional and alignment accuracy with respect to the feed structure as well as it required special equipment for lithography process, X-ray lithography.

In this Letter, we introduce a photolithographically definable polymer–ceramic composite that can be used to manufacture MMW DRAs with required small dimensions (a few millimetres) and accurate placement. The developed photolithographically definable composite allows manufacturing various complex DRA shapes using conventional ultraviolet (UV) photolithography instead of using an X-ray lithography. In this Letter, SU-8 2150 has been used as the polymer base, this polymer has high viscosity and required a different way to handle comparing with had been used by Rashidian *et al.* in the direct method, and alumina (Al_2O_3) nanopowder has been used as a nanofiller to increase the dielectric constant of the polymer. The SU-8–Al_2O_3 composite was photolithographically processed in cylinder shape with heights up to 350–500 μm, the required dimensions of W-band MMWs DRA. The SU-8–Al_2O_3 composite with this height is photo-definable using through mask UV-lithography to allow the designer to pattern the desired shapes with a precise position directly on a feed structure. Substrate penetration lithography has been used in this Letter to determine the maximum heights that can be processed for the different Al_2O_3 nanofillers content in the composite. The sidewalls of the processed structures were also studied to find out the dependence of their sharpness on the processing parameters and composite mixture. Prototype capacitors were fabricated and utilised to measure the SU-8–Al_2O_3 composites' relative dielectric permittivity and the result was compared with predicted

doi: 10.1049/mnl.2015.0389

values using the Lichteneker–Rother model that is the most commonly employed for two phase materials [11, 14–16]. Moreover, double layer patterning was demonstrated to enable more manufacturing flexibility for structures having high dielectric constant.

2. Fabrication technique and discussions

2.1. Synthesis of the SU-8–Al_2O_3 composite: The negative photoresist SU-8, used as the polymer in this Letter, was obtained from MicroChem. The SU-8 2000, a new generation of SU-8 photoresist, is formulated using cyclopentanone as solvent. This series demonstrates improved coating and adhesion properties and faster processing times for thick film applications. Photoresist films up to 650 µm thick can be easily spun using a conventional spin coater in a single coating process and photolithographically patterned using UV (350–400 nm) radiation [17]. Alumina-alpha (Al_2O_3) nanopowder, from MK Nano, with an average particle size of 40 nm is used as a ceramic nanofiller to increase the relative dielectric permittivity of the SU-8 photoresist.

The SU-8–Al_2O_3 composite samples have been prepared using the mechanical disperser IKA T10. The preparation starts by filling a 12 ml cylinder with half the amount of the SU-8 2150 photoresist to be used. The Al_2O_3 nanofiller and the remaining half of the resist are added alternately little by little to minimise agglomeration of the Al_2O_3 in the solution. The combination is initially mixed with guided hand stirring using the disperser shaft for 5 min to spread the nanopowder all over the solution. The mechanical disperser mixing of the nanocomposite blend follows in several steps; each step consists of 5 min mixing and 3 min cooling to prevent overheating of the solution and the disperser. The total mixing durations to reach homogeneous solution for the different Al_2O_3 contents in the SU-8–Al_2O_3 composite are listed in Table 1. The prepared SU-8–Al_2O_3 composite is then poured in a 10 ml syringe and left for 20 h in an upright position to allow the slow escape of trapped air bubbles from the viscous solution.

2.2. Film patterning results: Thorough and systematic investigations were carried out to find out the maximum thickness of SU-8–Al_2O_3 composite that can be polymerised by the UV light exposure in the lithography process. The objective of these investigations is to ascertain the limits of lithographically patterning SU-8–Al_2O_3 composite. Quartz substrates and back side exposure lithography were used for this purpose. In addition, the lateral sharpness of the cylindrical structure walls was studied using conventional photolithography on silicon (Si) substrates to determine the sidewall inclination angle of the fabricated structures as a function of the Al_2O_3 nanofiller percentage.

SU-8–Al_2O_3 composite mixtures with different concentrations of Al_2O_3 nanopowder were processed on quartz and Si substrates. Each substrate piece has a dimension of 2 cm × 2 cm. The substrates pieces were cleaned using acetone, and then rinsed with isopropyl alcohol. After that the quartz pieces were blown dry with dry N_2 and dehydrated on hot plate for 6 min at 200°C. Then 2 ml of the SU-8–Al_2O_3 composite mixture was injected from the syringe over the whole piece. Before spinning, the specimens were left for 3 min to allow uniform distribution of mixture over the quartz wafer pieces. Spinning was done in the two steps: in the first step, the wafer was accelerated at 100 rotations per minute (rpm)/s to a speed of 500 rpm for 8 s to allow the SU-8–Al_2O_3 composite to be spread over whole wafer. In the second step, each wafer was accelerated at 400 rpm/s to a known speed to get a suitable thickness for each specific experiment. To avoid thermal shock for the nanocomposite film during baking, the specimens' temperature were gradually increased during soft baking using two different hot plates, so the specimens were placed on the first hot plate at 50°C for 10 min and after that the specimens were placed on the second hot plate at 95°C for 108 min. The specimens were removed from the hot plate and allowed to cool down to approximately 20°C, and then the structures were patterned using photolithography. The specimens were then post baked using two hot plates the first at 50°C for 5 min, the second at 95°C for 28 min. Next, the specimens were developed for 20 min using SU-8 developer aided by hand stirring, and then rinsed in isopropyl alcohol; Fig. 1 shows a scanning electron microscope (SEM) micrograph of the processed dielectric cylinders after development.

Table 1 Mixing time against weight percentage for SU-8–Al_2O_3 composite samples

Al_2O_3, wt%	Mixing time, min
10	80
15	80
25	100
35	100

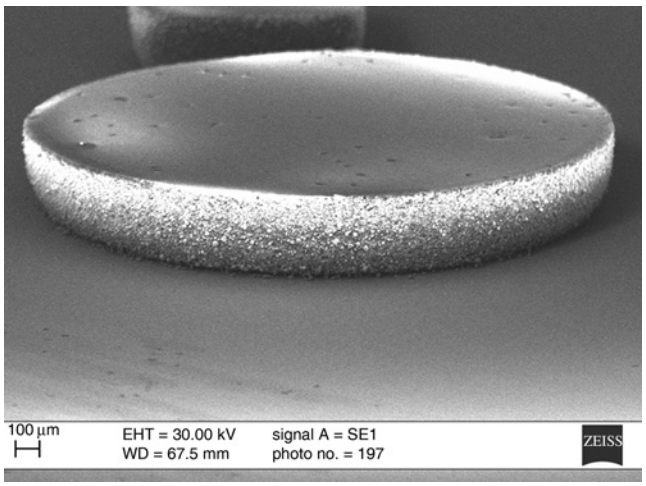

Fig. 1 *SEM micrograph for an SU-8–Al_2O_3 composite cylindrical dielectric structure fabricated on Si*

By utilising the back side exposure photolithography technique, Fig. 2, we expect that only polymerised part of the composite remains whilst the non-polymerised part will be rinsed out along with the developer and so the maximum polymeriseable thickness against content can be measured. All samples on quartz substrate were exposed to a fixed dose of 4.536 J/cm^2 for all mixture compositions.

The thickness of the structures after exposure and development was measured using Veeco Dektak 150 surface profilometer. For the purpose of comparison and to reach conclusive deductions of Al_2O_3 nanopowder effects on the maximum polymerised thickness pure SU-8 photoresist was first processed. It was found that an exposure dose of 387 mJ/cm^2 was enough to polymerise SU-8 photoresist films of thicknesses up to 800 µm. Fig. 3 shows the dependence of the maximum polymerised thickness against Al_2O_3 nanopowder content in the SU-8–Al_2O_3 composite mixture, the maximum thickness that can be polymerised gradually decreases with an increase in the weight percentage of Al_2O_3 in the SU-8–Al_2O_3 composite mixture. This reduction is due to an increase in resist absorption coefficient and its surface reflectance caused by the presence of the Al_2O_3 nanoparticles in the SU-8 film [18, 19].

Conventional photolithography, Fig. 4, was used to study the lateral sharpness of the walls of the cylindrical structures. The exposure dose that is required to polymerise the maximum thickness was optimised depending on the Al_2O_3 nanofiller content in the SU-8–Al_2O_3 composite mixture for the different samples. The maximum fabrication tolerances were seen in composites with an

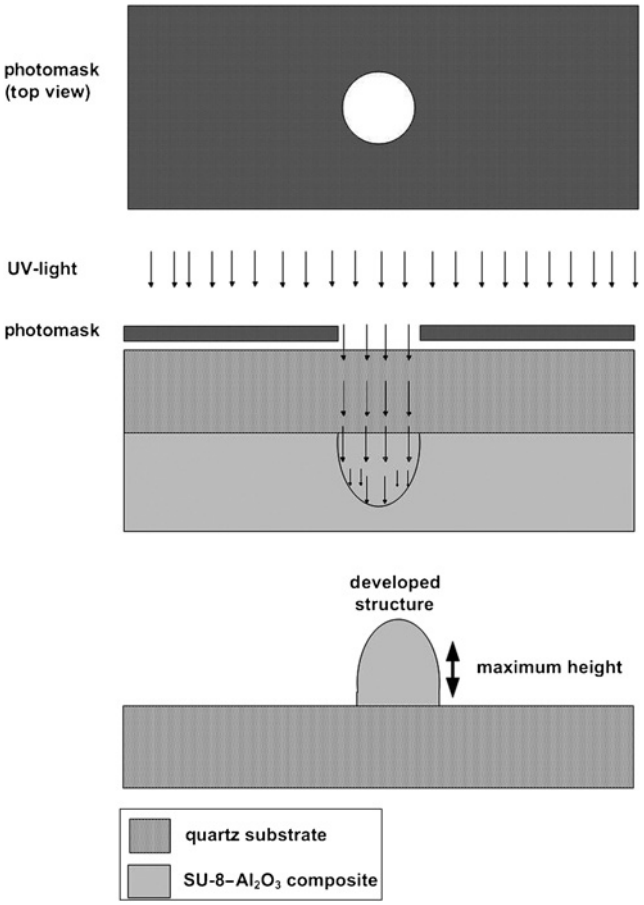

Fig. 2 *2D schematic of substrate penetration lithography process*

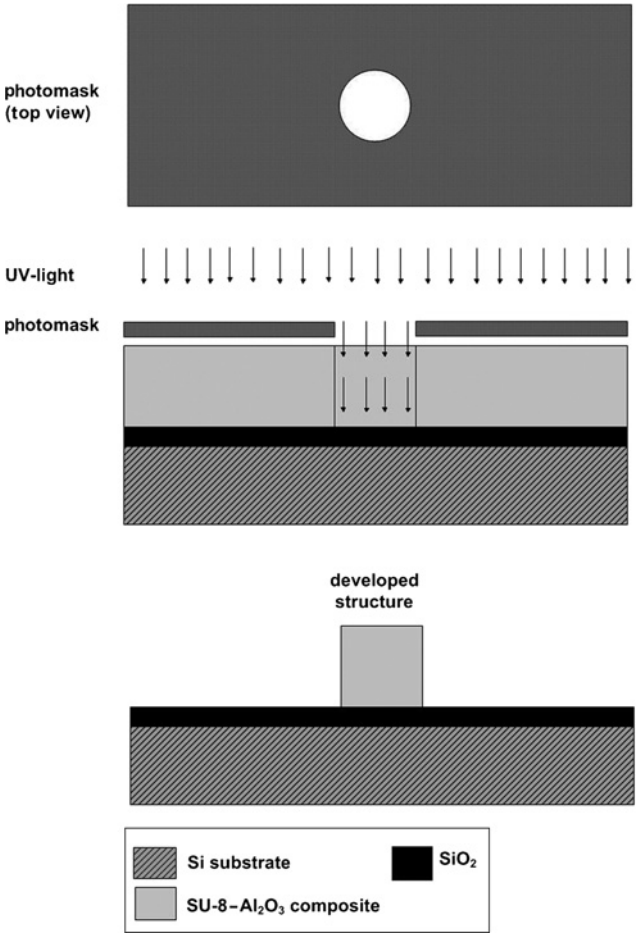

Fig. 4 *2D schematic of conventional lithography process used for fabricating cylindrical dielectric structures*

Al_2O_3 of 35 wt%. Cylinders fabricated with a photomask having 3 mm circular window exhibited an average top diameter of 3.2 ± 0.1 mm and an average thickness of 203 ± 10 µm.

Figs. 5–8 show SEM micrographs of the wall profile of the patterned structures fabricated during this Letter. The pure SU-8 photoresist structure, Fig. 5 shows satisfactorily straight sidewall, whereas the SU-8–Al_2O_3 composite mixture, Figs. 6–8 exhibit slanted profile.

Owing to the dependence of antenna characteristics on the shape and dimensions of the DRA structures, it is essential to investigate the reproducibility of such profile in order to design DRA antennas with predictable performance. Various SU-8–Al_2O_3 composite mixtures with different weight percentages of Al_2O_3 nanopowder were studied. Increasing the weight percentage of Al_2O_3 in the nanocomposite resists results in increasing inclination of the sidewalls. In addition, nearly all processed SU-8–Al_2O_3 composite mixture samples show two noticeably apparent sidewall regions. The first region is a thin layer at the upper part of the photoresist having an almost straight sidewall with an inclination angle smaller than 5°. The thickness of this first region depends strongly on the Al_2O_3 weight percentage content in the SU-8–Al_2O_3 composite, Table 2 lists the evaluated thickness of this region for the

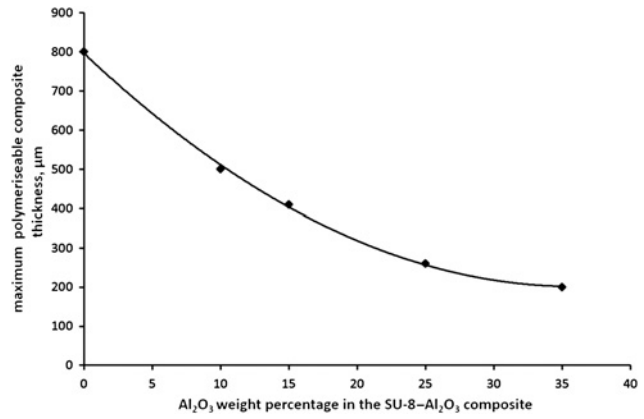

Fig. 3 *Evolution of the maximum polymeriseable thickness of SU-8–Al_2O_3 composite against Al_2O_3 weight percentage in the composite*

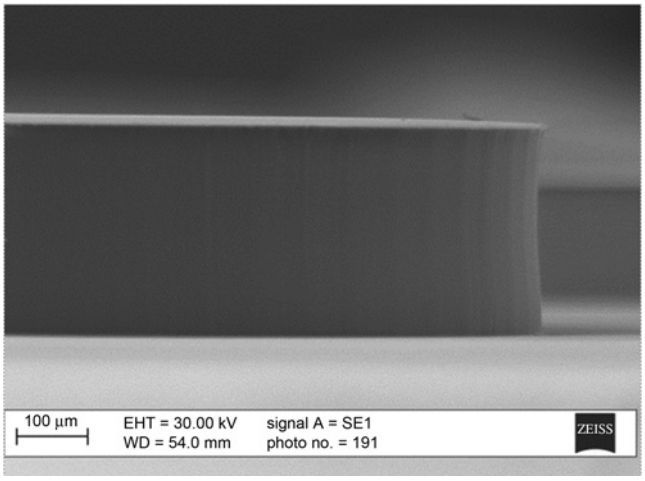

Fig. 5 *Film cross-section of pure SU-8. Cylindrical structures with 300 µm in height almost show a straight sidewall profile*

doi: 10.1049/mnl.2015.0389

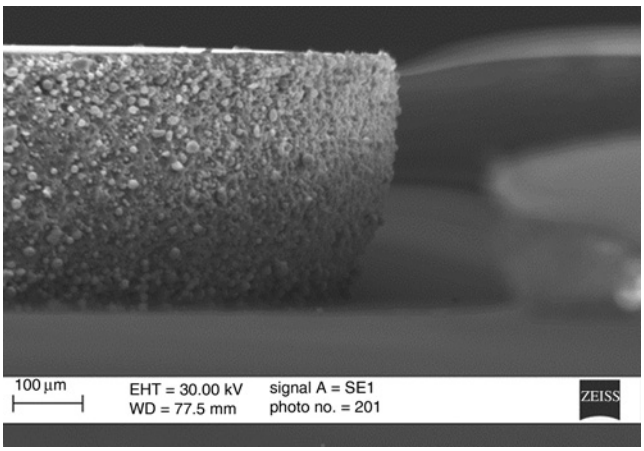

Fig. 6 *Film cross-section of SU-8–Al_2O_3 composite with an Al_2O_3 of 15 wt %. Two regions sidewall profile start to appear clearly; the first top region with sidewall angle less than 5° and the second region with sidewall angle greater than 5°*

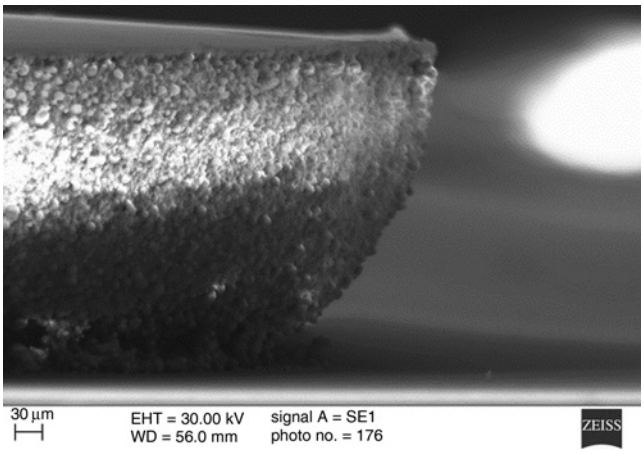

Fig. 7 *Film cross-section of SU-8–Al_2O_3 composite with an Al_2O_3 of 25 wt %. The first sidewall profile region with an angle less than 5° shrunk in compare with the second region with an angle greater than 5°*

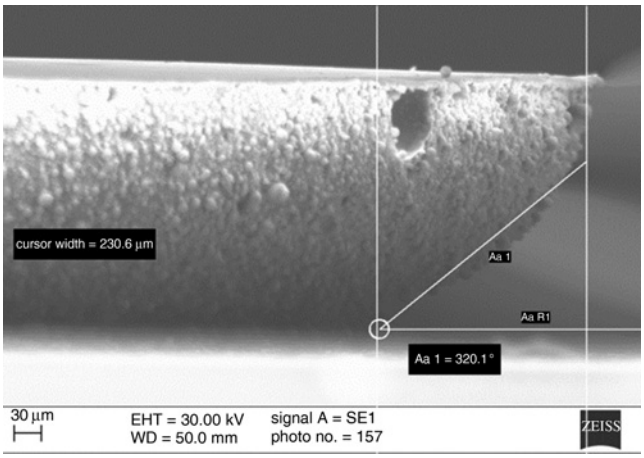

Fig. 8 *Film cross-section of SU-8–Al_2O_3 composite with an Al_2O_3 of 35 wt %. The sidewall profile region with an angle greater than 5° is dominant*

different Al_2O_3 weight percentages. The second region, with a much higher sidewall inclination extends up to the maximum possible thickness that can be processed. Mask edge diffraction effects

Table 2 Maximum polymeriseable film thickness for different Al_2O_3 weight percentages with side wall angle less than 5°

Al_2O_3, wt%	Maximum thickness, µm
10	~300
15	~200
25	~150
35	~90

are thought to be the main cause of these inclinations observed in our processed samples as reported in other work [20, 21]. Diffraction phenomenon is divided into three types; near field image, Fresnel diffraction and Fraunhofer diffraction. These types appear at increasing distance from the mask, respectively. For near image diffraction, the exposed resist have almost the same mask pattern, this region is very thin and cannot be seen in our samples. The Fresnel diffraction leads to a decrease in the UV light intensity at the edges causing the first inclination region observed in our samples. Deeper in the SU-8 mixture the UV light become of a Fraunhofer diffraction type, in which the light is focused at the centre of the mask opening and decays steadily towards the edges causing the resist to have a much higher sidewall inclination because of the gradient in the light intensity. These findings should be taken into account during the antenna design process. In Section 2.3, the double layer processing of the SU-8–Al_2O_3 composite was investigated as a solution to overcome the flexibility limitation and the undesired slant sidewall.

2.3. Double layer patterning: In the previous section, the maximum height limit for different SU-8–Al_2O_3 composites with different weight percentages has been determined as well as the unsatisfactory achievable sidewall profiles were revealed. In MMW application, DRAs are required to have structures with accurate shape and dimensions to avoid the frequency shifts [8]. Therefore, the sidewall angle observed in the lower region of the previously processed structures is undesirable. Furthermore, manufacturing flexibility required to fabricate DRA with higher dielectric constant in a single casted layer is limited by the maximum film thickness that have been specified in Fig. 3.

In this section, the double layer processing of the SU-8–Al_2O_3 composite was investigated as a solution to overcome the flexibility limitation and the undesired slant sidewall. A double layer of the SU-8–Al_2O_3 composite with an Al_2O_3 of 25 wt% is fabricated in order to realise structures with thicknesses higher than 150 µm

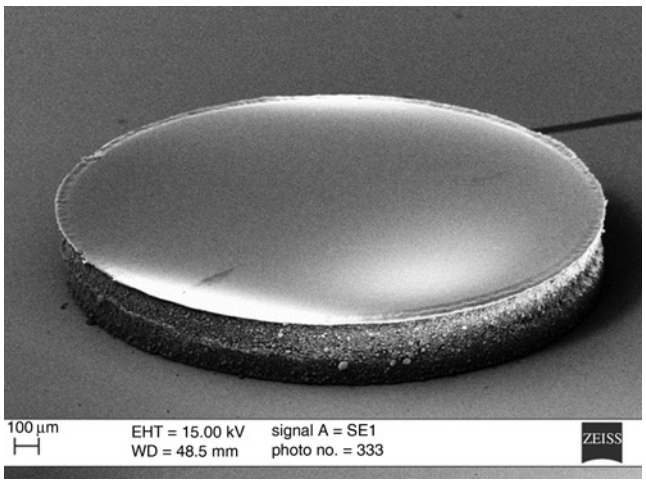

Fig. 9 *Patterned double layer patterned of SU-8–Al_2O_3 composite cylinder with an Al_2O_3 of 25 wt%. The total height is 385 µm*

and with the first region having a side wall profile less than 5°. The fabrication of a double layer of the SU-8–Al_2O_3 composite was realised by performing two consecutive coating and exposure steps using the same procedure described in Sections 2.1 and 2.2, but a single developing step has been applied at the end, Fig. 9 shows an SEM micrograph for a double layer SU-8–Al_2O_3 composite cylinder. The average measured thickness for a number of cylinders was ~385 µm with almost straight side wall profile. It was not easy to add more layers using this technique. The number of layers is limited by the alignment issue of the added layer with respect to the previous two layers as it will be difficult to see clearly the alignment marks through the previous two spun layers which contain the ceramic nanoparticles.

3. Dielectric constant study: The material dielectric permittivity plays the main role in DRA size, coupling efficiency and bandwidth [2, 22, 23]. There are a number of methods to measure the materials relative permittivity at high frequencies [24]. In this work, the influence of adding Al_2O_3 nanofiller to the SU-8 photoresist was investigated by manufacturing prototype capacitors and evaluating the relative dielectric constant of the SU-8–Al_2O_3 composite mixtures using the well-defined relationship

$$C = \varepsilon_o \varepsilon_r \frac{A}{t} \tag{1}$$

where ε_o and ε_r are dielectric permittivity of free space and relative dielectric permittivity of the insulating dielectric layer, respectively, A and t are the area of the top metallic contact and thickness of insulating layer, respectively. The prototype capacitors were fabricated by placing the processed SU-8–Al_2O_3 composite between two metallic contacts. The second patterned Al plate of all capacitors has a dimension of 8 mm × 8 mm and the SU-8–Al_2O_3 composite film has an average thickness of 150 µm. The two-dimensional (2D) schematic of the capacitor fabrication process is shown in Fig. 10. The capacitance against voltage measurement was performed using a semiconductor device analyser at a frequency of 1 MHz. Table 3 lists the measured relative dielectric permittivities for the SU-8–Al_2O_3 composite with different Al_2O_3 weight percentages.

There are a number of numerical models to predicate an effective relative dielectric permittivity for two phase materials mixture, the most commonly used model is the Lichteneker–Rother model. The Lichteneker–Rother model determines the effective permittivity for two phase materials mixture based on the volume percentage and effective dielectric permittivity for each material. Lichteneker–Rother mixing law equation [3, 11, 16]

$$\log \varepsilon_c = B \cdot \log \varepsilon_1 + (1 - B) \cdot \log \varepsilon_2 \tag{2}$$

where ε_c is composite permittivity, ε_1 is SU-8 relative permittivity (4.5 measured), ε_2 is Al_2O_3 permittivity (~10), B is SU-8 volume

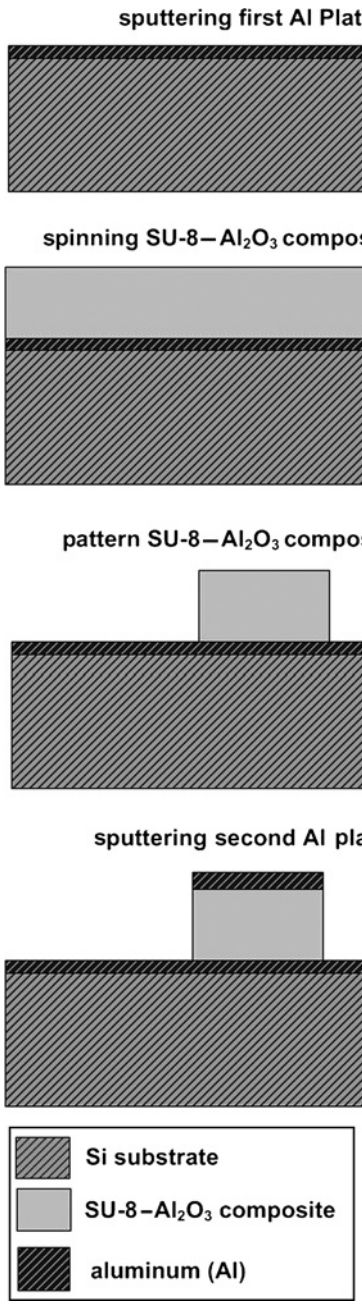

Fig. 10 *2D schematic of prototype capacitors fabrication steps. The capacitance of the capacitors were measured in order to calculate SU-8–Al_2O_3 composite relative permittivity*

Table 3 Measured relative dielectric permittivities for SU-8–Al_2O_3 composites with different Al_2O_3 weight percentages

Al_2O_3, wt%	Relative dielectric permittivity
0	4.5
10	4.8
15	4.97
25	5.17
35	5.66

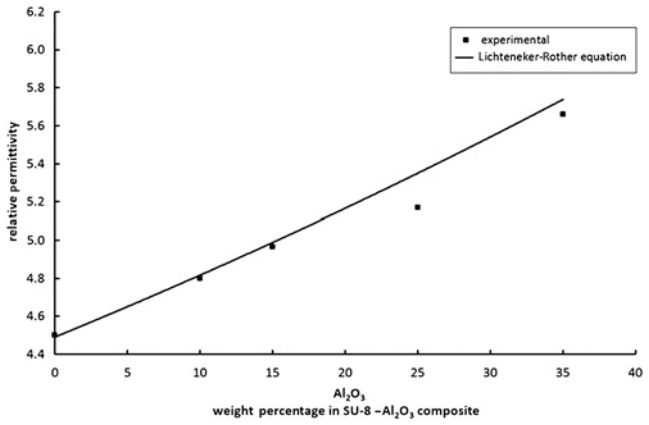

Fig. 11 *Experimental measured and theoretically predicted relative permittivity against to Al_2O_3 weight percent in the SU-8–Al_2O_3 composite*

doi: 10.1049/mnl.2015.0389

percentage, and $(1 - B)$ is Al_2O_3 volume percentage. Fig. 11 shows the comparison of the predicted and experimental relative permittivity of the SU-8–Al_2O_3 composite. The measured and predicted relative permittivities of the SU-8–Al_2O_3 composites show a trend of increasing with increasing the Al_2O_3 nanofiller weight percentage. The measured relative permittivity shows a small deviation from the predicted values.

4. Conclusions: Thick films of SU-8–Al_2O_3 composite with different Al_2O_3 nanofiller weight percentages were fabricated and investigated. The obtained composites remain UV-photodefinable and can be patterned for MMW DRAs up to a certain maximum film thickness. This maximum thickness was found to depend on the weight percentage of Al_2O_3 in the composite. The sidewall profile angle has been investigated for different Al_2O_3 percentages. The SU-8–Al_2O_3 composite dielectric constants were measured and compared with predicted values using Lichteneker–Rother equation, the measured permittivities of the SU-8–Al_2O_3 composite show a trend of increasing with increasing the Al_2O_3 nanofiller weight percentage. The double layer process of the SU-8–Al_2O_3 composite was developed to overcome some of the limitations in the single layer process; this process greatly increases the sidewall straightness of SU-8–Al_2O_3 composite structures and allows fabricating thicker structures. The relative permittivity of the developed composites, however, needs to be investigated at MMW frequencies using a W-band dielectric permittivity material measurement setup; and this is planned in our future work.

5. Acknowledgments: The authors extend their appreciation to the Deanship of Scientific Research at King Saud University for funding this work through the Research Project no NFG2-11-33.

6 References

[1] Petosa A.: 'Dielectric resonator antenna handbook' (Artech House, 2007, 3rd edn.)
[2] Luk K.M., Leung K.W.: 'Dielectric resonator antennas' (Research Studies Press, 2003)
[3] Xu J., Wong C.P.: 'High dielectric constant Su8 composite photoresist for embedded capacitors', *J. Appl. Polym. Sci.*, 2007, **103**, (3), pp. 1523–1528
[4] Ndieguene A., Campistron P., Carlier J., *ET AL.*: 'Su-8 photoresist and Su-8 based nanocomposites for broadband acoustical matching at 1 GHz', *J. Phys., Conf. Ser.*, 2009, **195**, (1), p. 012005
[5] Iyer G., Gorur R.S., Richert R., *ET AL.*: 'Evaluation of epoxy based nanodielectrics for high voltage outdoor insulation'. IEEE Int. Symp. on Electrical Insulation (ISEI), 2010
[6] Singha S., Thomas M.J.: 'Dielectric properties of epoxy–Al_2O_3 nanocomposite system for packaging applications', *IEEE Trans. Compon. Packag. Technol.*, 2010, **33**, (2), pp. 373–385
[7] Rashidian A., Klymyshyn D.M., Aligodarz M.T., *ET AL.*: 'Photoresist-based polymer resonator antennas with permanent frame', *Electron. Lett.*, 2012, **48**, (9), pp. 475–477
[8] Rashidian A., Klymyshyn D.M., Aligodarz M.T., *ET AL.*: 'Photoresist-based polymer resonator antennas: lithography fabrication, strip-fed excitation, and multimode operation', *IEEE Antennas Propag. Mag.*, 2011, **53**, (4), pp. 16–27
[9] George S., Raman S., Mohanan P., *ET AL.*: 'Polymer ceramic composites for microwave substrate and antenna applications'. A Workshop on Advanced Antenna Technology, 2010 Indian Antenna Week, 2010
[10] Rashidian A., Klymyshyn D.M., Boerner M., *ET AL.*: 'Deep X-ray lithography processing for batch fabrication of thick polymer-based antenna structures', *J. Micromech. Microeng.*, 2010, **20**, (2), p. 025026
[11] Qi W., Chen G., Alghamdi A.S.: 'Influence of nanofillers on electrical characteristics of epoxy resins insulation'. 10th IEEE Int. Conf. on Solid Dielectrics (ICSD), 2010
[12] Rashidian A., Aligodarz M.T., Klymyshyn D., *ET AL.*: 'Photoresist-based dielectric resonator antenna fabrication and performance: a review'. 16th Int. Symp. on IEEE Antenna Technology and Applied Electromagnetics (ANTEM), 2014
[13] Aligodarz M.T., Klymyshyn D.M., Rashidian A., *ET AL.*: 'Investigations on photoresist-based artificial dielectrics with tall-embedded metal grids and their resonator antenna application', *IEEE Trans. Antennas Propag.*, 2015, **63**, (9), pp. 3826–3838
[14] Rao Y., Wong C.P., Jianmin Q., *ET AL.*: 'Effective dielectric constant prediction of polymer-ceramic composite based on self-consistent theory'. 50th Electronic Components & Technology Conf., 2000
[15] Subodh G., Deepu V., Mohanan P., *ET AL.*: 'Dielectric response of high permittivity polymer ceramic composite with low loss tangent', *Appl. Phys. Lett.*, 2009, **95**, (6), pp. 062903
[16] Singha S., Thomas M.J.: 'Permittivity and tan delta characteristics of epoxy nanocomposites in the frequency range of 1 MHz–1 GHz', *IEEE Trans. Dielectr. Electr. Insul.*, 2008, **15**, (1), pp. 2–11
[17] 'Su-8 2000 processing guidlines', in MICHRO.CHEM (ed.), Secondary:Su-8 2000 Processing Guidelines
[18] Halloran M.L.G.a.J.W.: 'Scattering of ultraviolet radiation in turbid suspensions', *J. Appl. Phys.*, 1997, **81**, (6), p. 9
[19] Jiguet S., Bertsch A., Hofmann H., *ET AL.*: 'Su8-silver photosensitive nanocomposite', *Adv. Eng. Mater.*, 2004, **6**, (9), pp. 719–724
[20] Lawes R.A.: 'Manufacturing tolerances for Uv liga using Su-8 resist', *J. Micromech. Microeng.*, 2005, **15**, pp. 2198–2203
[21] Chuang Y.J., Tseng F.G., Lin W.K.: 'Reduction of diffraction effect of Uv exposure on Su-8 negative thick photoresist by air gap elimination', *Microsyst. Technol.*, 2002, **8**, (4), pp. 308–313
[22] Mongia R.K., Bhartia P.: 'Dielectric resonator antennas – a review and general design relations for resonant frequency and bandwidth', *Int. J. Microw. Millim.-Wave Comput.-Aided Eng.*, 1994, **4**, (3), pp. 230–247
[23] Rashidian A., Klymyshyn D.M., Tayfeh Aligodarz M., *ET AL.*: 'Development of polymer-based dielectric resonator antennas for millimeter-wave applications', *Progr. Electromagn. Res. C*, 2010, **13**, pp. 203–216
[24] Chen L.F., Ong C.K., Neo C.P., *ET AL.*: 'Microwave electronics: measurement and materials characterization' (John Wiley & Sons, 2005)